

matrix outside of 0.75 fm. This is illustrated in Fig. 9(b) of R. A. Bryan and B. L. Scott, Phys. Rev. **135**, B434 (1964), where we show that when the one-boson-exchange potential is set identically to zero within 0.75 fm, then  $\delta(^3D_1)$  varies only  $+2^\circ$ . This result has been confirmed by B. L'Oiseau (private communication) who finds a similar  $+2^\circ$  variation when he sets the potential of Lacombe *et al.* (Ref. 8) to zero within this distance. This variation is in the right direction, but  $\epsilon_1$  goes negative in disagreement with experiment. Furthermore, the misfit between theory and experiment is also evident at 142 MeV, and at this lower energy  $\delta(^3D_1)$  is insensitive to variations in the potential much farther out.

<sup>15</sup>Pion-production-threshold-energy dependence ne-

glected in Refs. 8 and 11 may not be sufficient to explain the  $^3D_1$  misfit because the trouble extends down to 142 MeV as well, as mentioned earlier and shown in Fig. 2; also any simultaneous increase in  $\delta(^3D_2)$  and  $\delta(^1D_2)$  of the magnitude required for  $\delta(^3D_1)$  will lead to unacceptably high  $\chi^2$  because the experimental limits on  $\delta(^1D_2)$  of are narrow and the theoretical  $\delta(^3D_2)$  is already too high. Selecting a larger  $s$ -wave  $\pi\pi \rightarrow N\bar{N}$  amplitude squared,  $|f_+^0|^2$ , to increase the effective " $\sigma$ " potential also will not work, again because it raises  $\delta(^1D_2)$  and  $\delta(^3D_2)$  along with  $\delta(^3D_1)$ . Increasing the  $\rho$ -resonance contribution will also probably not suffice because it is too weak at  $D$ -wave range, as shown in Fig. 1(j) of J. Binstock and R. Bryan, Phys. Rev. D **4**, 1341 (1971).

### Search for Narrow Neutral-Meson Resonances near Mass 1 GeV/c<sup>2</sup>\*

M. Buttram, H. B. Crawley, D. W. Duke,† R. C. Lamb, R. J. Leeper, and F. C. Peterson  
Ames Laboratory—ERDA and Department of Physics, Iowa State University, Ames, Iowa 50010

(Received 12 June 1975)

We examine the reaction  $\pi^-p \rightarrow X^0n$  at 2.4 GeV/c for evidence of the production of the previously reported narrow neutral mesons  $M^0(940)$ ,  $\delta(963)$ ,  $M^0(1033)$ , and  $M^0(1150)$ . Strong evidence against the existence of these states is presented.

Evidence for four new narrow meson resonances was reported<sup>1-3</sup> from a missing-mass (MM) experiment by an Iowa State University—Argonne National Laboratory—Purdue University collaboration studying the reaction  $\pi^-p \rightarrow X^0n$ . The MM is defined to be the  $X^0$  mass. Subsequent experiments by another group<sup>4-5</sup> have failed to confirm these resonances. In the present Letter we present the results of an experiment designed to reproduce the results of Refs. 1-3 as closely as possible with significantly more data and to have the ability, not present in Refs. 1-5, to reconstruct constrained final states.

The experiment was performed at the Argonne National Laboratory zero-gradient synchrotron. A plan view of the apparatus is shown in Fig. 1(a). Thirty plastic scintillator neutron detectors of the type employed in Refs. 1-3 (30 cm  $\times$  30 cm  $\times$  15 cm deep) were used in conjunction with a magnetostrictive-wire spark-chamber system, the effective-mass spectrometer<sup>6</sup> at the zero-gradient synchrotron. This Letter presents data not analyzed for constrained final states. For the present analysis the effective-mass spectrometer was used to measure the angles of any final-state charged particles passing through its front spark chambers K1 and K2. These data were taken at a  $\pi^-$ -beam momentum of 2.4 GeV/c and analyzed to

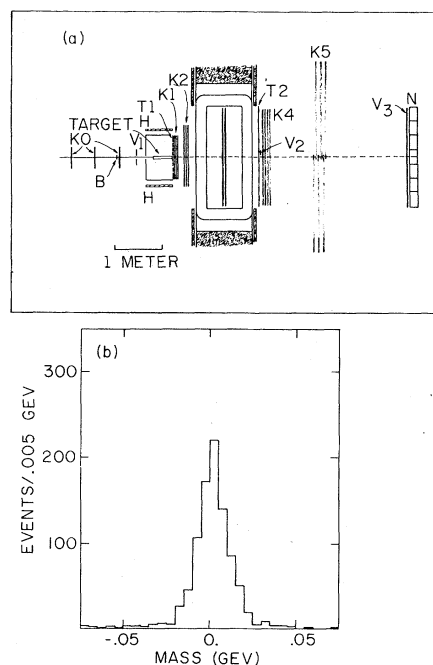


FIG. 1. (a) Plan view of the experimental layout. K0-K5 are magnetostrictive-wire spark chambers. B, V<sub>1</sub>, and V<sub>2</sub> are counters, T<sub>1</sub>, T<sub>2</sub>, H, and V<sub>3</sub> are hodoscopes, and N are the neutron detectors. (b) Histogram of the difference between the MM and the di-pion mass measured by the spectrometer for the reaction  $\pi^-p \rightarrow \pi^+\pi^-n$ .

$\pm 0.25\%$ . Neutrons were detected after a 5.33-m flight path from a 38.1-cm liquid-hydrogen target. The neutron detectors were arranged about the beam line in an array which intercepted neutron angles up to  $12.5^\circ$ . Only signals corresponding to neutrons with times of flight (TOF) in the interval 38 to 100 nsec were accepted. Such slow forward-going neutrons are produced very close to  $180^\circ$  from the beam direction in the reaction center-of-mass frame. For the geometry of this experiment and for  $X^0$  masses near  $1 \text{ GeV}/c^2$ ,  $|t - t_{\min}|$  is less than  $0.003 (\text{GeV}/c)^2$ . The MM, as calculated from the beam and neutron momenta, is almost independent of the neutron angle under these circumstances. The MM and its error are most sensitive to the neutron TOF measurement. The allowed TOF's for this experiment correspond to MM in the range  $0.85$  to  $1.25 \text{ GeV}/c^2$ . The MM resolution was  $\sigma = 0.004 \text{ GeV}/c^2$  at  $1 \text{ GeV}/c^2$ .

This experiment was designed to permit a reasonable reproduction, consistent with the addition of the spectrometer, of the charged-particle-multiplicity and angle cuts used to enhance the effects seen in Refs. 1-3. As previously mentioned, angles of forward-going particles were measured in the spectrometer's front chambers. For particles produced at wider angles a sixteen-counter hodoscope  $H$  surrounding the target gave an angular measure sufficient to reproduce the desired cuts. Outside of these counters was  $0.64 \text{ cm}$  of lead backed by an additional fourteen counters which were used to select events involving  $\gamma$  rays. Forward-going  $\gamma$  rays were detected in the neutron counters.

Between the target and the spark chambers was an eleven-counter hodoscope  $T1$  made of  $0.33 \text{ cm}$  scintillator which completed a  $4\pi$ -solid-angle detector about the target. A typical trigger required at least one particle in  $T1$ , at least one in a hodoscope  $T2$  following the magnet, an incident beam particle, and one and only one neutron counter signal in the allowed time interval. A potential event was vetoed if any particle was detected in the beam-halo counter  $V_1$ , the unreacted-beam veto counter  $V_2$ , or that element of the charged-particle veto hodoscope  $V_3$  covering the counter which detected the neutron. In order to avoid incorrect TOF data from the association of a neutron signal with the wrong beam particle, a potential event was eliminated if another beam particle arrived within 400 nsec of the beam particle of interest.

A total of  $33.5 \times 10^9$  beam particles yielded a set of  $2.58 \times 10^6$  events satisfying the trigger logic.

These events form a sample approximately 10 times that of Refs. 1-3. It should be noted that the requirement of one particle through the spectrometer provides an acceptance versus MM which is slightly different from that of Refs. 1-3. However for the present data this is not important as it will not bias a search for narrow structures.

The spectrometer was used to check the MM as calculated from beam and neutron parameters for the constrained final state  $\pi^+\pi^-n$ . This was possible because the spectrometer-alignment procedure decoupled its measurement of the  $X^0$  mass from the corresponding MM measurement. The difference between the two measurements is displayed in Fig. 1(b). Note that the position of the peak indicates that the two mass measurements agree within a few  $\text{MeV}/c^2$ . The width of the peak is consistent with the stated MM resolution ( $\sigma = 0.004 \text{ GeV}/c^2$ ) and the expected spectrometer resolution ( $\sigma = 0.007 \text{ GeV}/c^2$ ). A two-dimensional histogram (not shown) of MM versus spectrometer mass shows that there is no systematic variation between the two mass scales over the range of the experiment.

In Fig. 2(a) we present our mass spectrum with

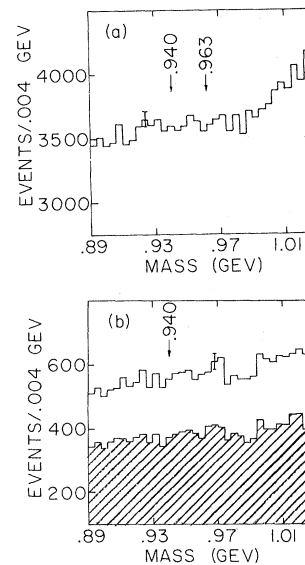


FIG. 2. (a) Histogram of the MM for events with two charged particles, one with  $0^\circ < \theta_{\text{lab}} < 17^\circ$  and the other with  $17^\circ < \theta_{\text{lab}} < 100^\circ$ . (b) Subsets of the events in (a) which cannot result from two-pion decays of the  $X^0$ . The shaded events have a  $\gamma$  ray and an azimuthal-angle difference ( $\Delta\phi$ ) between  $147$  and  $180^\circ$ . The unshaded events include the shaded events plus events with  $0^\circ < \Delta\phi < 33^\circ$ .

cuts equivalent to those applied to produce the spectrum in Fig. 3(b) of Ref. 1. Two resonances were reported in Ref. 1, the  $M^0(940)$  and the  $\delta(963)$ . Both were seen in final states involving two charged particles. The  $M^0(940)$  was seen in final states containing missing neutrals. The  $\delta(963)$  was not seen in final states containing missing neutrals. Events in Fig. 2(a) contain two charged particles in the final state, one with  $0^\circ < \theta_{lab} < 17^\circ$  and the other with  $\theta_{lab} > 17^\circ$ , where  $\theta$  is the polar angle. In Fig. 2(b) we present subsets of the data in Fig. 2(a) which cannot be the result of two-body decays. The shaded portion of the figure contains events for which the difference in azimuthal angles between the two charged particles  $\Delta\phi$  lies in the range  $147$  to  $180^\circ$  but which also have a  $\gamma$  in the final state. The unshaded portion of Fig. 2(b) contains the shaded portion plus events with  $0^\circ < \Delta\phi < 33^\circ$ . No evidence is ap-

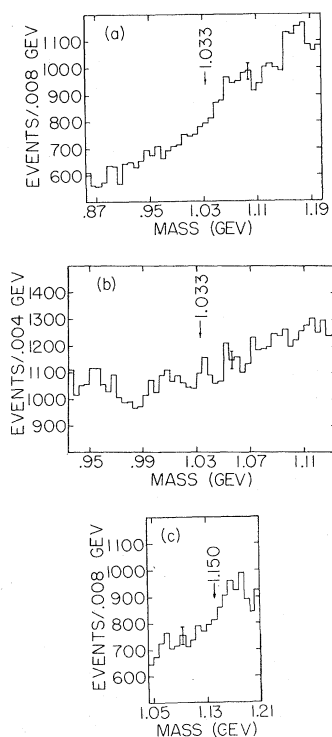


FIG. 3. (a) Histogram of the MM for two-charge events with one polar angle less than  $17^\circ$  and the other in the range  $6.5$  to  $17^\circ$ . The azimuthal-angle difference  $\Delta\phi$  is between  $79$  and  $180^\circ$ . (b) Two-charge events with polar angles in the ranges  $6.5^\circ < \theta_1 < 17^\circ$  and  $17^\circ < \theta_2 < 100^\circ$  and with  $\Delta\phi$  in the range  $169^\circ < \Delta\phi < 180^\circ$ . The cuts for (a) and (b) enrich the data in pure dimeson final states. (c) Two-charge events with both polar angles in the range  $0^\circ < \theta < 17^\circ$  and  $79^\circ < \Delta\phi < 146^\circ$ . These cuts eliminate pure dimeson final states.

parent in either figure for the  $M^0(940)$  or  $\delta(963)$ .

In Fig. 3(a) we present our mass spectrum which is equivalent to Fig. 2(a) of Ref. 2. Events in Fig. 3(a) have two charged particles in the final state with  $79^\circ < \Delta\phi < 180^\circ$  and the larger polar angle between  $11$  and  $17^\circ$ . Figure 3(b) which reproduces Fig. 2(c) of Ref. 2 shows two-charged-particle events with  $169^\circ < \Delta\phi < 180^\circ$  and one polar angle in the range  $6.5$  to  $17^\circ$  while the other polar angle is greater than  $17^\circ$ . Neither spectrum shows evidence for the  $M^0(1033)$ .

In Fig. 3(c) we present our mass spectrum equivalent to Fig. 3(b) of Ref. 3 which reported the resonance  $M^0(1150)$ . The  $M^0(1150)$  was seen in final states involving two charged particles after removal of pure two-body final states. Events in Fig. 3(c) have two charges,  $79^\circ < \Delta\phi < 146^\circ$ , and both polar angles less than  $17^\circ$ . Again there is no evidence for the  $M^0(1150)$ .

As a measure of the disparity between the present results and those of Refs. 1–3, we present in Table I estimates of the number of events we would have expected based on the published production cross sections  $d\sigma/dt$  for these four mesons at  $0^\circ$  (column 2 of Table I). The number of expected events (column 3) is given by

$$N = \rho A L B \epsilon (d\sigma/dt) \Delta t, \quad (1)$$

where  $\rho$  is the density of liquid hydrogen ( $0.0708 \text{ g/cm}^3$ ),  $A$  is Avagadro's number,  $L$  is the target length ( $38.1 \text{ cm}$ ), and  $B$  is the total beam ( $33.5 \times 10^9 \pi^-$ ). The momentum-transfer interval  $\Delta t$  is

TABLE I. The number of events (column 3) we would have expected for the mesons listed in column 1 assuming their production cross sections as given in Refs. 1–3. These differential cross sections at polar angle ( $\theta$ ) equal to zero are given in column 2.

Meson	$(d\sigma/dt)_{\theta=0}$ [mb/(GeV/c) <sup>2</sup> ]	Number of events expected <sup>a</sup>
$M^0(940)$	0.52	3300 [Fig. 2(a)]
$\delta(963)$	0.49	3600 [Fig. 2(a)]
$M^0(1033)$	0.07	860 [Fig. 3(a)]
	0.22	2600 [Fig. 3(b)]
$M^0(1150)$	0.025	670 [Fig. 3(c)]

<sup>a</sup> A fraction of the data (39%) was obtained with a trigger which suppressed the detection of events satisfying the cuts of Figs. 2(a) and 3(a). The corresponding numbers given in column 3 do not include any correction for this suppression. The size of the correction is at most 39%.

the range of the square of the four-momentum transfers corresponding to the neutron angles subtended by the neutron counters. The efficiency  $\epsilon$  is the product of three terms. The first is the detection probability of a neutron in a 15-cm-thick neutron counter,  $18 \pm 4\%$ .

The second term is the probability of getting one charged particle through the spectrometer as required by our trigger. For this factor which depends on the decay mode of the  $X^0$  we use an estimate of 33% based on Monte Carlo studies of dipion decays. From  $Q$ -value considerations higher-multiplicity final states give a larger value for this acceptance leading to larger expected event estimates which are in even greater disagreement with the present data.

The third and final factor in the efficiency is the probability that the decay products of the  $X^0$  will satisfy the angle cuts. As in Refs. 1-3, we take this probability to be unity. The justification for this procedure in Refs. 1-3 was that the only significant effect of the cuts imposed was to reduce the background level under the respective signals.

With the assumptions given above we calculate the number of events expected (column 3 of Table I) for each of the four mesons and observe that there is no evidence for effects of this magnitude in any of the figures. We believe that if the cross sections of Refs. 1-3 were correct we would have seen obvious effects. We therefore conclude on the basis of an event sample approximately 10 times larger than but otherwise very similar to

that of Refs. 1-3 that there is no evidence for the production of the  $M^0(940)$ ,  $\delta(963)$ ,  $M^0(1033)$ , or  $M^0(1150)$  in our reaction. This confirms the results of Refs. 4 and 5.

We wish to thank the staff of the zero-gradient synchrotron for their fine support. Special thanks are due to the effective-mass-spectrometer group.

---

\*Research supported by the U. S. Energy Research and Development Administration under Contract No. W-7405-eng-82.

†Present address: Department of Physics and Astronomy, University of Rochester, Rochester, N. Y. 14627.

<sup>1</sup>D. L. Cheshire, R. W. Jacobel, R. C. Lamb, F. C. Peterson, E. W. Hoffman, and A. F. Garfinkel, *Phys. Rev. Lett.* **28**, 520 (1972).

<sup>2</sup>A. F. Garfinkel, E. W. Hoffman, R. W. Jacobel, D. L. Cheshire, R. C. Lamb, and F. C. Peterson, *Phys. Rev. Lett.* **29**, 1477 (1972).

<sup>3</sup>R. W. Jacobel, D. L. Cheshire, R. C. Lamb, F. C. Peterson, A. F. Garfinkel, and E. W. Hoffman, *Phys. Rev. Lett.* **29**, 671 (1972).

<sup>4</sup>D. M. Binnie, L. Camilleri, A. Duane, D. A. Garbutt, J. R. Holmes, W. G. Jones, J. Keyne, M. Lewis, I. Siotis, P. N. Upadhyay, I. F. Burton, and J. G. McEwen, *Phys. Lett.* **39B**, 275 (1972).

<sup>5</sup>D. M. Binnie, L. Camilleri, J. Carr, N. C. Debenham, A. Duane, D. A. Garbutt, W. G. Jones, J. Keyne, I. Siotis, and J. G. McEwen, *Phys. Rev. Lett.* **32**, 392 (1974).

<sup>6</sup>D. S. Ayres, ANL Report No. ANL/HEP 7314, 1973 (unpublished).

<sup>7</sup>The analysis of constrained final states will be published later.

---

## Optical-Model Analysis of N + C and C + C Elastic Scattering\*

John S. Eck, J. H. Johnson,† D. O. Elliott,‡ and W. J. Thompson§  
*Department of Physics, Kansas State University, Manhattan, Kansas 66506*  
 (Received 14 July 1975)

Additional data and optical-model calculations for  $^{14}\text{N}+^{12}\text{C}$  elastic scattering which expand and fortify the recently published optical-model analysis of N + C and C + C elastic scattering by Delic are discussed.

We have recently measured and analyzed elastic scattering excitation functions of  $^{14}\text{N}+^{12}\text{C}$  at six center-of-mass angles between  $55^\circ$  and  $120^\circ$  at  $^{14}\text{N}$  bombarding energies between 15.0 and 25.0 MeV (corresponding to 6.92 through 11.5 MeV in the center of mass). Four angular distributions were measured at center-of-mass energies 6.92,

9.23, 9.92, and 10.85 MeV in the angular range from  $\theta_{c.m.} = 20^\circ$  to  $135^\circ$ .

The main emphases in our work were threefold: (1) search for any nonstatistical structures in the excitation functions; (2) study the compound contributions to the elastic scattering cross sections; (3) perform a detailed optical-model analysis for